Excitation functions of pion single charge exchange reactions in ^{27}Al, ^{45}Sc, and ^{65}Cu

R. S. Rundberg, B. J. Dropesky, G. C. Giesler, and G. W. Butler
Isotope and Nuclear Chemistry Division, Los Alamos National Laboratory, Los Alamos, New Mexico 87545

S. B. Kaufman and E. P. Steinberg
Chemistry Division, Argonne National Laboratory, Argonne, Illinois 60439
(Received 5 April 1984)

The cross sections for the pion single charge exchange reactions $^{27}Al(\pi^-,\pi^0)^{27}Mg$, $^{45}Sc(\pi^+,\pi^0)^{45}Ti$, and $^{65}Cu(\pi^-,\pi^0)^{65}Ni$ were measured at pion kinetic energies from 80 to 400 MeV by activation techniques. The excitation functions measured for these target nuclei do not show any structure near the (3,3) resonance, but rather, all exhibit a monotonic decrease in cross section over this energy range, proportional to T_π^{-1}. Theoretical predictions based on the impulse approximation with the Fermi gas model show a minimum near the (3,3) resonance, in disagreement with these experimental results.

I. INTRODUCTION

Pion single charge exchange (SCE) reactions have received considerable attention recently, both experimentally and theoretically.[1] The early measurements[2] of excitation functions for SCE reactions were done using the activation method, and were of the (π^+,π^0) reaction on ^{7}Li, ^{10}B, and ^{13}C. The latter case was of particular interest because the product, ^{13}N, has only one particle-stable state, the ground state, which is the isobaric analog of the target nucleus, making it more amenable to theory. The cross section for the $^{13}C(\pi^+,\pi^0)^{13}N$ reaction was approximately constant over the energy range 70—250 MeV, with a value of about 1.0 mb. The excitation functions for the other two targets were similar in shape and had magnitudes of about 2.5 mb for ^{7}Li and 0.4 mb for ^{10}B.

Calculations based on the plane-wave impulse approximation predicted a maximum in the cross section near the energy of the (3,3) resonance, while calculations which included absorption (multiple scattering or distorted wave) predicted a minimum in this energy region. A recent calculation[3] using the delta-hole formalism was able to reproduce the flat experimental shape, but the magnitude was about a factor of 3 low.

More recent experiments have studied the SCE reaction by detecting the coincident γ rays from the π^0 decay. One such experiment[4] measured the excitation functions at a forward angle for the $^7Li(\pi^+,\pi^0)$ and $^{13}C(\pi^+,\pi^0)$ reactions. In contrast to the angle-integrated activation results, the cross sections rose rapidly between 70 and 150 MeV, and were almost constant between 150 and 180 MeV.

In order to extend the data on SCE excitation functions to heavier nuclei, we have determined the cross sections for the reactions $^{27}Al(\pi^-,\pi^0)^{27}Mg$(9.4 min), $^{45}Sc(\pi^+,\pi^0)^{45}Ti$(3.1 h), and $^{65}Cu(\pi^-,\pi^0)^{65}Ni$(2.5 h) for pion energies in the range 80—400 MeV. These reactions populate many final states in the product nuclei, in contrast to the light nuclei previously studied, for which only a few states are particle stable. An appropriate model with which to compare the present data is the Fermi-gas model, which has been used[5] to calculate the excitation function for the pion SCE reaction $^{65}Cu(\pi^-,\pi^0)^{65}Ni$. The results of the present measurements will be compared with calculations according to this model.

II. EXPERIMENTAL

A. Pion irradiations and radioactivity measurements

The targets were irradiated with beams of pions from the P^3 channel at LAMPF for energies above 100 MeV, and from the low-energy pion (LEP) channel for 100 MeV and lower energies. The momentum spread ($\Delta p/p$) of the beam was $\pm 8\%$ in the P^3 channel and $\pm 4\%$ in the LEP channel. The lengths of the irradiations varied with the target; the aluminum targets were irradiated for 20 min (approximately two half-lives of ^{27}Mg), and the scandium and copper targets for 1.5—6 h. The fluctuations of beam intensity during each irradiation were recorded to permit the calculated cross sections to be corrected for such variations.

The pion intensity was determined by activation of Al monitor foils to produce 110-min ^{18}F and 15-h ^{24}Na. Three aluminum foils were irradiated simultaneously, the center foil being the monitor and the outer foils serving to compensate for recoil loss and gain by the center foil. The aluminum targets used for determining the pion SCE cross sections required no additional monitor foils. The excitation functions for the production of ^{18}F and ^{24}Na from aluminum have been measured at LAMPF (Ref. 6) relative to the absolute cross sections for the $^{12}C(\pi^\pm,\pi N)^{11}C$ reactions.[7] The π^+ beam was estimated to contain $<2\%$ proton contamination at 300 MeV, and $<1\%$ at lower energies.

The ^{18}F disintegration rates in the Al monitor foils were determined by γ-γ coincidence counting of the annihilation radiation with a pair of 7.6 cm $\times$ 7.6 cm NaI(Tl) scintillators. This counting system was calibrated periodically with activated Pilot B scintillator disks whose ^{11}C

absolute positron disintegration rates had been determined by β^+-γ coincidence counting (see Ref. 7 for a more detailed description of the counting system).

The ^{24}Na disintegration rates of the Al monitor foils used for the longer runs were determined by gamma counting with a calibrated Ge(Li) spectrometer. The Ge(Li) detectors were calibrated using a National Bureau of Standards (NBS) mixed γ-ray standard source. The NBS standard was a point source; therefore the efficiency was corrected for the effect of an extended source by mapping out the shape of the beam spot and taking a weighted average of the measured efficiencies. The decay data of the individual samples were analyzed by the least-squares program CLSQ.[8]

The aluminum targets were 3.8-cm-diam disks of 99.999% purity, ranging in thickness from 36 to 216 mg/cm^2, so that the effect of secondary reactions could be studied (see the following). The targets were brought to a low-background environment within 5 min after each irradiation and counted on either of two shielded Ge(Li) γ spectrometers in the LAMPF Nuclear Chemistry Laboratory; the 843.8-keV γ ray was used to determine the ^{27}Mg yield. The samples were counted for 30 min to 1 h.

The ^{27}Mg activity produced via the secondary reaction, ^{27}Al(n,p)^{27}Mg, was determined by measuring the apparent cross section as a function of target thickness. Measurements were made using at least three thicknesses of aluminum foil at each pion energy. The pion intensities were determined by measuring the ^{18}F produced in the target foils; this spallation product is presumed to be free of secondary reaction contributions. The ^{18}F activity in the aluminum targets was counted with the γ-γ annihilation counter already described.

The scandium targets were high-purity metal targets 2.54-cm square; the thickness of the targets was varied in order to determine the magnitude of the secondary effect. After irradiation in the pion beam, these targets were dissolved in dilute 3*M* HCl. Ten milligrams of Ti carrier as $TiCl_3$ was then added and the solution warmed to ensure complete exchange. Ten milliliters of 6% cupferron solution was added to complex the Ti^{3+} and form a titanium cupferrate precipitate. The cupferrate was then extracted into chloroform which had been pretreated with 3*M* HCl, and the chloroform was then washed two times with 3*M* HCl. The chloroform was then evaporated, and the cupferron destroyed with nitric acid and hot sulfuric acid. Finally, the titanium was again precipitated with cupferron. The cupferrate was filtered out and mounted on a counting plate. This procedure was tested prior to the pion experiment by irradiating scandium foils with 800-MeV protons. The procedure was shown to be effective in eliminating scandium activity. Titanium-45 is a 3.08-h pure positron emitter, so its activity was determined, after chemical separation, with the same γ-γ annihilation counters used to count ^{18}F. The decay of the ^{45}Ti activity was followed over periods of 12 h and longer, and the decay data were fit with the least-squares program CLSQ, which provided the activities extrapolated to the end of bombardment. Also, the half-lives determined from CLSQ were used as a further check to ensure the purity of the ^{45}Ti product.

After counting the titanium samples, the chemical yield was determined spectrophotometrically. The samples were dissolved with nitric and perchloric acids. To these solutions was added 1 ml of hydrogen peroxide to form pertitanic acid which is strongly colored; they were analyzed against standards prepared from the original stock solution that was used for the Ti carrier.

The copper targets consisted of metallic foils of two types: natural isotopic abundance, and foils enriched in ^{65}Cu to an abundance of 99.7%. The latter foils were used as "thin" targets (10 mg/cm^2) to study the effect of target thickness, and were also used in a stack of comparable thickness to the foils of natural copper to increase the amount of ^{65}Ni activity.

A chemical procedure was designed to separate Ni from the much larger concentration of Cu and purify it radiochemically from the spallation products present at much higher activity levels. The specificity of dimethylglyoxime (DMG) for Ni was used for both separation and purification, along with steps for the elimination of possible contaminants. The Cu target was dissolved in dilute HNO_3 in the presence of Ni carrier and small amounts of Fe(III) and Mn(II). This solution was made basic with NH_4OH, precipitating $Fe(OH)_3$. About 0.2 g of $(NH_4)_2C_2O_4$ was then added in order to prevent Mn from coprecipitating with the Ni in the following step, because tests had shown the presence of ^{56}Mn contamination in the final product if this was omitted. An excess of DMG in alcoholic solution was added to precipitate the NiDMG compound. After washing, the precipitate was dissolved in dilute HNO_3, a few milligrams of Cu added, and CuS precipitated by passing H_2S through the solution. The H_2S was removed from the liquid by boiling, and Ni was again precipitated from the basic solution as the DMG compound. The chemical yield was determined by weighing and was usually 70—90%.

The Ni samples were counted using low-background beta counters. The efficiency of these counters for detecting ^{65}Ni was determined as a function of sample thickness by means of a series of standardized sources of ^{65}Ni. They were prepared by neutron irradiation of natural Ni, and were standardized by measuring the intensity of the 1481.9-keV γ ray with a calibrated Ge(Li) spectrometer. The decay curves were resolved into two components of half-lives 2.52 h and 36.0 h, corresponding to ^{65}Ni and ^{57}Ni, respectively.

B. Secondary reactions in the targets

The radionuclides formed by pion single charge exchange reactions can also be formed by the analogous nucleon charge exchange reaction, caused by the secondary nucleons produced in the target by the pion beam. Thus, the (π^-,π^0) and (n,p) reactions result in the same product, as do the (π^+,π^0) and (p,n) reactions. The contribution of such secondary reactions to the observed yield can be estimated by measuring the apparent cross section as a function of target thickness and extrapolating to zero thickness. The most suitable measure of target thickness for this purpose is the mean path length of the secondary particles in the target, since the yield should be propor-

tional to this quantity. A simple relationship between the mean path length of secondary neutrons and the target dimensions has been derived[9] for production from a point source in the center of a circular target of radius r and thickness of $t \ll r$. Further assumptions for secondary neutrons are that they are formed isotropically and there is no attenuation due to absorption in the target. The mean path length, $\bar{l}$, is then given by

$$\bar{l} = \frac{t}{2}\left[\frac{3}{2} - \ln\frac{t}{r}\right] . \quad (1)$$

The most extensive measurements of the secondary effect were made for the aluminum targets, for which the effect of the (n,p) reaction was large. Measurements of the cross section for ^{27}Mg formation were made for three target thicknesses at all pion energies studied. The data from measurements at 160, 200, and 300 MeV are shown in Fig. 1 as a function of mean path length, with least-squares linear fits at each pion energy to arrive at the zero thickness intercept, which we take to be the (π^-,π^0) cross section. The magnitude of the secondary effect (the slopes of the lines) varies with the beam energy, decreasing by nearly a factor of 2 in going from 160 to 300 MeV. This may be due to a larger neutron production cross section in the vicinity of the (3,3) resonance and a decrease in the (n,p) cross section with energy.

The magnitude of the secondary effect for the formation of ^{65}Ni in Cu targets via the (n,p) reaction was measured at pion energies of 200 and 300 MeV. The thin target consisted of enriched ^{65}Cu, 10-mg/cm^2 thick, plus the 7-mg/cm^2 Al monitor, while the thick target was 90-mg/cm^2 Cu and 30-mg/cm^2 Al. The difference in apparent cross sections was 16 ± 20 μb at 200 MeV, and 54 ± 20 μb at 300 MeV; in terms of the mean path length from Eq. (1), the average correction is 0.13 ± 0.07 μb/mg cm^{-2}. This slope is much smaller than those for aluminum targets as shown in Fig. 1. The reason lies in the magnitude of the (n,p) cross sections involved, with the ^{27}Al(n,p) reaction having about five times the cross section of the ^{65}Cu(n,p) reaction between 10- and 20-MeV neutron energy.[9] Similar differences in the secondary effects for these two targets were observed for protons of several GeV energy.[10,11]

The contribution of the secondary (p,n) reaction to the formation of ^{45}Ti in the Sc targets is more difficult to determine because of the short effective range of the secondary protons. A study of the formation cross section for ^{45}Ti with 180-MeV π^+ in Sc targets differing by a factor of 3.5 in total thickness (target plus monitor foils) was carried out. The targets consisted of a thin one of 7.6 mg/cm^2 Sc, an intermediate one of 36.8 mg/cm^2, and the thickest one of 80 mg/cm^2, plus a 24 mg/cm^2 Al monitor foil packet immediately downstream of each Sc target. The measured cross sections were corrected for secondary ^{45}Ti production using the method described in the Appendix. The largest correction for the 80-mg/cm^2 target was

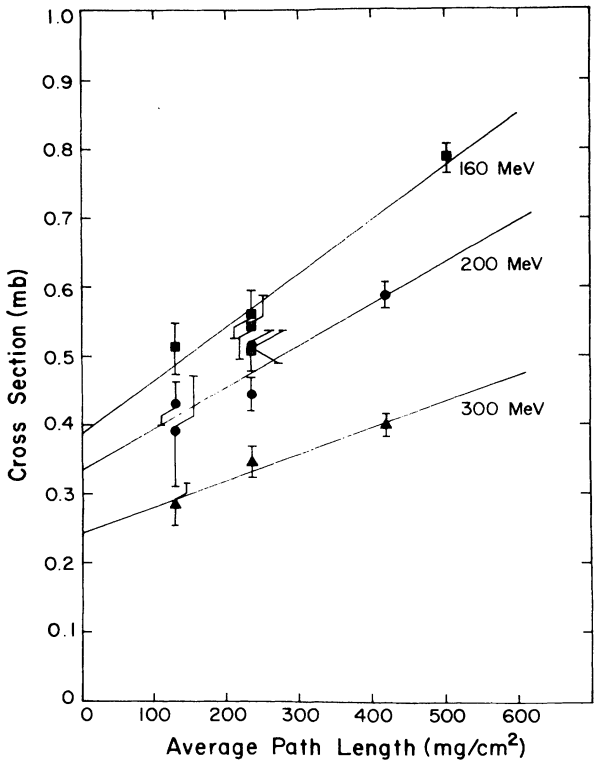

FIG. 1. Apparent cross sections for the ^{27}Al$(\pi^-,\pi^0)^{27}$Mg reaction at 160, 200, and 300 MeV as a function of secondary neutron average path length in Al target foils.

TABLE I. Secondary corrections for the ^{45}Sc$(\pi^+,\pi^0)^{45}$Ti.

Pion energy (MeV)	Target thickness (mg/cm^2) Sc + Al	Uncorrected cross section (μb)	Secondary contribution (μb)	Corrected cross section (μb)
100	80 + 24	2049	167	1882
180	7.4 + 24	996	89	907
	37 + 24	1142	161	981
	80 + 24	1144	225	919
300	37 + 24	691[a]	175	516
	80 + 124	708	244	465

[a]Average of two measurements.

20%. After correction, the values for the three thicknesses were scattered about the mean with a standard deviation of 4%. This is a smaller deviation than the distribution of uncorrected data (7%). It should be noted, however, that these deviations are smaller than the uncertainty due to counting statistics and the estimated uncertainty in the chemical yield determinations (8%). The corrections applied at all energies and target thicknesses are given in Table I. An increase in the uncorrected cross section with target thickness was observed for both 180- and 300-MeV π^+. This increase is not evident in the corrected cross sections. However, as already noted, the secondary corrections are generally small compared to the scatter in the data.

III. RESULTS AND DISCUSSION

The results of these measurements are given in Table II, as cross sections for each of the pion SCE reactions studied, corrected for secondary effects. The errors given in Table II include the uncertainty in the monitor cross sections, as well as the uncertainties arising from counting statistics, decay-curve resolution, and detector efficiency calibration.

These data are shown in Fig. 2 as a function of pion kinetic energy, together with curves obtained from the calculations according to Kaufman and Hower.[5] This calculation addresses the question of activation measurements on medium-mass nuclei, in particular the ^{65}Cu(π^-,π^0)^{65}Ni reaction. The reaction is assumed to occur as a quasifree pion-nucleon charge exchange,

$$\pi^- + p \rightarrow n + \pi^0 , \quad (2)$$

with the restriction that the neutron be bound in the residual nucleus. Furthermore, the excitation energy of that nucleus, equal to the sum of the proton hole and neutron particle energies, must not be large enough to allow particle evaporation, otherwise the ^{65}Ni product would not result. Thus, only a small fraction of the total charge-exchange cross section is effective in forming the observed radiochemical product.

The Fermi-gas model was used to evaluate the density of particle-stable final states, and distortion effects were included in an approximate way by integrating the product of the pion-nucleon cross section and the nuclear density along the pion's path.[12] Straight-line trajectories were assumed, and both pion-nucleon scattering (modified by the Pauli Principle) and pion absorption were included. The distortion effects resulted in a minimum in the cross section near the (3,3) resonance, owing to the strong absorption of the incoming and outgoing pion waves. The calculated excitation function for the (π^-,π^0) reaction was found to be proportional to ZE_0^2/A, where E_0 is the maximum excitation energy in the residual nucleus and Z

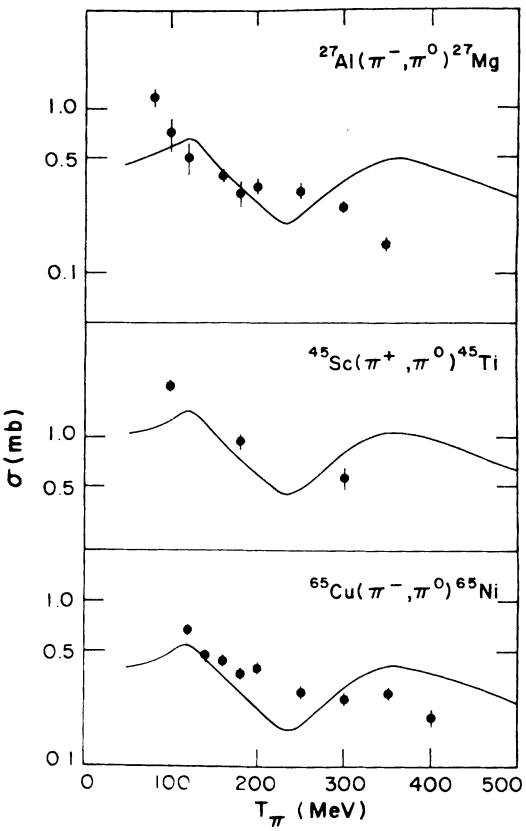

FIG. 2. Excitation functions of the pion SCE reactions ^{27}Al(π^-,π^0)^{27}Mg, ^{45}Sc(π^+,π^0)^{45}Ti, and ^{65}Cu(π^-,π^0)^{65}Ni. The smooth curves are the calculations according to the method of Kaufman and Hower (Ref. 5).

TABLE II. Cross sections for pion single charge exchange reactions.

Pion energy (MeV)	^{27}Al(π^-,π^0)^{27}Mg σ (μb)	^{45}Sc(π^+,π^0)^{45}Ti σ (μb)	^{65}Cu(π^-,π^0)^{65}Ni σ (μb)
80	1178±186		
100	716±180	1882±141	
120	505±117		660±56
140			470±36
160	397±33		442±47
180	306±59	936±112	369±34
200	343±32		396±31
250	314±32		285±31
300	250±18	499±87	259±26
350	149±14		280±30
400			200±25

and A are the atomic number and mass number of the target.

Since the calculation in Ref. 5 was specifically for the ^{65}Cu nucleus, the published excitation function can be scaled according to the above-mentioned factor for the targets. The inverse-A dependence results from the nuclear volume dependence of the distortion effects. For a (π^+,π^0) reaction, the elementary process (2) becomes $\pi^+ + n \rightarrow p + \pi^0$, and the cross section is proportional to the number of neutrons rather than Z. The primary variation of cross section for different targets is due to the variation of E_0.

For calculating the curves shown in Fig. 2, a Fermi momentum of 280 MeV/c was used, and the values of E_0 used were equal to the neutron binding energy plus 1.0 MeV. The experimental data show none of the structure predicted by the model, but rather appear to have a smoothly decreasing cross section with pion kinetic energy. The calculated cross sections are of the correct order of magnitude, however, and the predicted dependence on E_0 is confirmed by the data. Thus, ^{27}Mg and ^{65}Ni have similar neutron binding energies, 6.44 MeV and 6.10 MeV, respectively, and their cross sections are similar in magnitude. On the other hand, the neutron binding energy in ^{45}Ti is 9.42 MeV, and its cross section is 2—3 times larger than that of the former nuclides.

The experimental excitation functions, with their smoothly decreasing cross sections, suggest an inverse dependence on the incident pion kinetic energy. This type of energy dependence has been observed recently[13] in the ^{7}Li(p,n)^{7}Be charge exchange reaction in a similar energy range, as well as in (p,xn) reactions[14,15] on targets such as ^{197}Au and ^{209}Bi. In Fig. 3, the data are plotted on a log-log scale, and lines corresponding to a T_π^{-1} dependence are shown. It is clear that such an energy dependence fits the data rather well over the energy range 80—400 MeV. One can understand this qualitatively for nucleon charge exchange reactions[16] in terms of a single energy-independent nucleon-nucleon interaction and the requirement that the captured nucleon be in a small, fixed-energy window, while the total phase space increases with the available energy. However, it is difficult to apply such a picture to explain the present results for pion charge exchange, since both the primary reaction (2) and the distortion effects are strongly energy dependent.

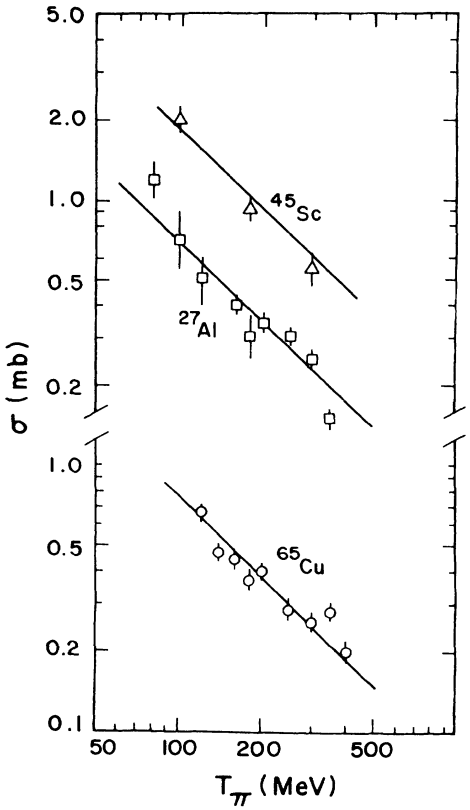

FIG. 3. Cross sections of the three studied pion SCE reactions, compared to lines corresponding to a T_π^{-1} energy dependence.

Excitation functions[2] for (π^+,π^0) reactions on the light nuclei ^{7}Li, ^{10}Be, and ^{13}C do not show this inverse energy dependence, but are rather flat between 70 and 250 MeV. The cross sections do decrease above 150 MeV, but less rapidly than as T_π^{-1}. Thus, there appears to be a change in the energy dependence of the $(\pi^\pm,\pi^0)$ reactions when the number of excited states populated in the final nucleus becomes large.

In summary, the excitation functions for pion SCE reactions leading to multiple bound states in the region of the (3,3) resonance do not show any structure, but rather decrease smoothly with pion energy, approximately as T_π^{-1}. This may result from a broadening of the resonance inside the nucleus, causing the predicted structure to be washed out.

ACKNOWLEDGMENTS

We gratefully acknowledge the work of the LAMPF technical staff and operating crews for enabling us to carry out these target irradiations. Our gratitude is expressed to W. R. Gibbs, J. J. Berlijn, and L.-C. Liu for many helpful discussions and calculations relevant to our experimental results. This research was performed under the auspices of the Office of High Energy and Nuclear Physics, Division of Nuclear Physics, U.S. Department of Energy.

APPENDIX: CORRECTION FOR SECONDARY (p,n) REACTION

The secondary production of ^{45}Ti due to the ^{45}Sc(p,n)^{45}Ti reaction caused by protons produced in the target was calculated using the following formulae[17] which take into account the geometry of the targets and energy loss in the target.

For a target thickness t less than the proton interaction range R, the secondary yield is

$$\langle Y(t,E_p)\rangle = \frac{t}{2R}\int_0^{R_p} n\sigma(u)du + \frac{1}{t}\int_0^t C(x)dx\ , \quad \text{(A1)}$$

where R_p is the proton range in the target material;[18] E_p is the proton energy; n is the number of target nuclei per unit volume; σ is the secondary reaction cross section as a function of the proton path length, μ, in the target, i.e.,

the excitation function is expressed in terms of the distance required to degrade the initial proton energy to a given energy; and

$$C(x)=\int_{\theta_R}^{\pi/2} F(x,\theta)\cos\theta\, d\theta \tag{A2}$$

and

$$F(x,\theta)=\int_0^{x/\sin\theta} n\sigma(u)du\ . \tag{A3}$$

The first term in this expression is the yield due to protons which can never leave the target. The second term is the yield due to protons which are able to leave the target and is expressed in terms of the yields due to protons leaving the target in the backward direction, $F(x,\theta)$.

For $t > R$, the secondary yield is

$$\langle Y(t,E_p)\rangle=\left[1-\frac{R}{2t}\right]\int_0^{R_p} n\sigma(u)du+\frac{1}{t}\int_0^{R} C(x)dx\ , \tag{A4}$$

and for continuity at $t=R$, the yield is

$$\langle Y(R,E_p)\rangle=\tfrac{1}{2}\int_0^{R_p} n\sigma(u)du+\frac{1}{R}\int_0^{R} C(x)dx\ . \tag{A5}$$

The secondary yield was determined by integration[19] over the proton energy distribution calculated[20] by the intranuclear cascade code ISOBAR (Ref. 21) for π^+ interactions with ^{45}Sc at 100-, 180-, and 300-MeV incident energies. The secondary yield due to protons evaporated from the excited nuclei after the intranuclear cascade was also calculated[19] by integrating over the proton energy distribution calculated by the Dostrovsky, Fraenkel, and Friedlander (DFF) (Ref. 22) evaporation code. Experimental cross sections for the ^{45}Sc(p,n)^{45}Ti reaction as a function of proton energy were used in these calculations and came from the work of Dell *et al.*[23] and McGee *et al.*[24] The total yields of ^{45}Ti secondary production for the three pion energies are plotted in Fig. 4 as a function of target thickness. Note that the secondary effect becomes nearly constant for thick targets. This saturation effect is due to the finite range of secondary protons in the target material. This correction makes it impossible to determine empirically the secondary correction by measuring the cross section as a function of target thickness when thick targets are required.

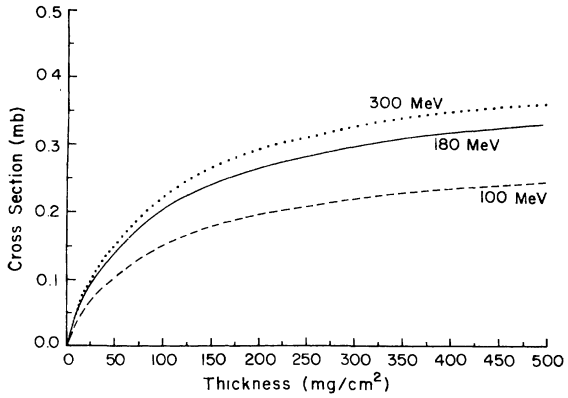

FIG. 4. Calculated secondary production of ^{45}Ti via the (p,n) reaction associated with the reaction ^{45}Sc(π^+,π^0)^{45}Ti.

In addition to secondary reactions resulting from protons produced within the scandium target, there is a secondary contribution resulting from protons produced in the aluminum monitor foils. The proton production intensity is nearly independent of the target material because it is primarily dependent on the proton density of the target material. The protons are emitted almost isotropically, and the range for protons at energies low enough to produce ^{45}Ti is short. Therefore, the secondary contribution from protons produced in the aluminum monitor foil can be approximated using the secondary cross section for scandium. However, only protons emitted in the backward hemisphere will interact with the scandium target. Therefore, the secondary contribution from the monitor foil is calculated as one-half the secondary cross section for a scandium target having a thickness equal to the monitor foil thickness (in mg/cm^2). The total calculated secondary contribution was subtracted from the experimental cross section to arrive at the corrected SCE cross sections reported here.

[1]For a review, see J. Alster and J. Warszawski, Phys. Rep. **52**, 87 (1979), and references therein.
[2]Y. Shamai, J. Alster, D. Ashery, S. Cochavi, M. A. Moinester, A. I. Yavin, E. D. Arthur, and D. M. Drake, Phys. Rev. Lett. **36**, 82 (1976).
[3]M. Hirata, Phys. Rev. C **24**, 1604 (1981).
[4]A. Doron *et al.*, Phys. Rev. Lett. **48**, 989 (1982).
[5]S. B. Kaufman and C. O. Hower, Phys. Rev. **140**, B1272 (1965).
[6]B. J. Dropesky, G. W. Butler, G. C. Giesler, C. J. Orth, and R. A. Williams, to be submitted to Phys. Rev. C.
[7]B. J. Dropesky, G. W. Butler, C. J. Orth, R. A. Williams, M. A. Yates-Williams, G. Friedlander, and S. B. Kaufman, Phys. Rev. C **20**, 1844 (1979).
[8]J. B. Cumming, U.S. AEC Report NAS-NA-3017, 1963, p. 25.
[9]D. I. Garber and R. R. Kinsey, Neutron Cross Sections, Vol. II, Resonance Parameters, 3rd ed., edited by S. F. Mughabghab, M. Divadeenam, and N. E. Holden, Brookhaven National Laboratory Report BNL-325, (1976).
[10]L. P. Remsberg, Phys. Rev. **138**, B572 (1965).
[11]A. M. Poskanzer, J. B. Cumming, and L. P. Remsberg, Phys. Rev. **168**, 1331 (1968).
[12]T. Ericson, F. Selleri, and R. T. Van de Walle, Nucl. Phys. **36**, 353 (1962).
[13]T. E. Ward, C. C. Foster, G. E. Walker, J. Rapaport, and C. A. Goulding, Phys. Rev. C **25**, 762 (1982).
[14]S. B. Kaufman and E. P. Steinberg, Phys. Rev. C **22**, 167 (1980).
[15]T. E. Ward, P. P. Singh, D. L. Friesel, A. Yavin, A. Doron, J. M. D'Auria, G. Sheffer, and M. Dillig, Phys. Rev. C **24**, 588

(1981).
[16]J. R. Grover and A. A. Caretto, Annu. Rev. Nucl. Sci. **14**, 51 (1964).
[17]J. J. Berlijn, private communication.
[18]*Hydrogen Stopping Powers and Ranges in All Elements,* edited by H. Andersen and J. Ziegler (Pergamon, New York, 1977), Vol. III.
[19]W. R. Gibbs, private communication.
[20]L.-C. Liu, private communication.
[21]G. D. Harp, K. Chen, G. Friedlander, Z. Fraenkel, and J. M. Miller, Phys. Rev. C **8**, 851 (1973); J. N. Ginocchio, *ibid.* **17**, 195 (1978).
[22]I. Dostrovsky, Z. Fraenkel, and G. Friedlander, Phys. Rev. **116**, 683 (1959).
[23]G. F. Dell, W. D. Ploughe, and H. J. Hausman, Nucl. Phys. **64**, 513 (1965).
[24]T. McGee, C. L. Rao, G. B. Saha, and L. Yaffe, Nucl. Phys. **A150**, 11 (1970).